Gravity Based Autonomous Calibration for Robot Manipulators

Donghai Ma, John M. Hollerbach and Yangming Xu

Biorobotics Laboratory, McGill University
3775 University St., Montreal, Quebec H3A 2B4

Abstract

This paper presents an autonomous method to calibrate joint torque sensors for advanced robots; as a by-product, the position sensors can also be calibrated. When one joint of a manipulator is rotated, the gravity torque exerted on the joint varies sinusoidally with rotation angle. By means of sinusoidal curve fitting, the bias of the torque sensor and the gain of the position sensor can be found directly. The gravity vector, expressed in the defined base coordinates, can also be found. Thereafter we determine the torque sensor gain as well as the rotation angle offset, by attaching a known load to robot in different positions. Experimental results are shown for the first two joints of the Sarcos Dextrous Arm.

1 Introduction

Joint torque information is required in inertial parameter identification and model-based control [1]; it may even be used for kinematic calibration [7]. While joint torque sensing continues to be a problem for robots, the advent of robot manipulators with high resolution joint torque and position sensors makes many algorithms practical [9]. To achieve best performance, the internal robot model should be calibrated periodically. This includes the calibration of joint torque sensors, for both gain and offset.

Calibrating joint torque sensors usually requires tedious human involvement. To find the torque sensor bias of a joint, one method is to manually adjust the bias so that the joint moves freely to align itself with gravity [11]; this method is somewhat qualitative. For the torque sensor gain calibration, hanging a mass on a known lever arm is the usual method. For autonomous robots, these procedures are certainly not the ideal ones. A calibration procedure for six axial force sensors has been proposed in [6]. However, to our knowledge, this paper is the first one to address the problem of autonomous calibration of the joint torque sensors.

Knowing the gravity vector $\mathbf{g}$ is another important issue for robot control; this knowledge is also required for our calibration method. Because $\mathbf{g}$ is always pointing down, it may be taken for granted that $\mathbf{g}$ is already known well enough and that its direction is along one axis of the world coordinates. Yet the floor surface or robot base plate may not be perfectly perpendicular to the gravity vector. This makes solving for the gravity vector an important topic. In this paper, we show a method to find $\mathbf{g}$ with the intrinsic joint torque and position sensors of a manipulator.

We assume that the arm has been previously calibrated for kinematic parameters; we have implemented several different schemes on our Sarcos Dextrous Arm [3, 5, 7]. An interesting by-product of our torque sensor calibration method is that the joint angle sensor gains and offsets can also be calibrated. Although the accuracy of this approach probably will not reach that possible with traditional kinematic calibration methods [10], we present it as an option. Unlike the fixed geometric parameters such as link lengths and joint axis orientations, the joint sensor gains and offsets often have to be recalibrated periodically. Especially in the context of teleoperation, high accuracy for the joint sensor gains and offsets may not be necessary and the procedure presented here can be adequate.

The procedures proposed in this paper involve the static rotation of the robot joints, and are summarized below.

1. We calibrate the torque sensor bias and position sensor gain from the sinusoidal relationship between the joint torque and rotation angle.

2. The gravity vector in the base coordinates is found from the amplitude and phase information of two sinusoidal curves when observing the coordinated rotations of the first two joints.

3. The torque sensor gain and position sensor bias are calibrated from the proximal joint to the distal joint. To provide an absolute reference, a special endpoint fixture is employed involving a load with known inertial parameters, moved to two positions.

A knowledge of the gravity vector is required for the third step. In the third step, manual intervention is required to move the load into two relatively known positions, but it is not necessary to know how this load is attached to the endpoint. This procedure does not identify the characteristics of the most distal joint; other procedures will have to be implemented for this determination. Experimental results are shown for the first two joints of the Sarcos Dextrous Arm.

2 Method

The Denavit-Hartenberg (D-H) convention [4] for joint i is used.

$\mathbf{z}_{i-1}$ is the rotation axis for joint i,

$\mathbf{x}_i$ is the common normal between $\mathbf{z}_{i-1}$ and $\mathbf{z}_i$,

i	α_j (deg)	θ_j^{off} (deg)
1	90.0	0.0
2	-90.0	135.0

Table 1: Nominal D-H parameters of Sarcos Dextrous Arm.

θ_i is the rotation angle between $\mathbf{x}_{i-1}$ and $\mathbf{x}_i$ about $\mathbf{z}_{i-1}$, and

α_i is the skew angle between $\mathbf{z}_{i-1}$ and $\mathbf{z}_i$ about $\mathbf{x}_i$.

We define the base coordinates in such a way that there will be no joint angle offset for the first joint, i.e., $\theta_1 = 0$, when joint 1 is at one mechanical limit stop. The rotation matrix that transforms link i coordinates to link $i-1$ coordinates is:

$$^{i-1}R_i = \begin{bmatrix} c\theta_i & -s\theta_i c\alpha_i & s\theta_i s\alpha_i \\ s\theta_i & c\theta_i c\alpha_i & -c\theta_i s\alpha_i \\ 0 & s\alpha_i & c\alpha_i \end{bmatrix} \tag{1}$$

where the abbreviations are $s\alpha_i = sin(\alpha_i)$, $c\theta_i = cos(\theta_i)$, etc. The nominal D-H parameters of the first two joints of the Sarcos Dextrous Arm are given in Table 1.

Here we assume that the skew angle α_i is known from the manufacturer's specification or from previous kinematic calibration results. The equations for the joint torque sensing and joint angle sensing are shown below:

$$\tau_i = \tau_i^{gain}\tau_{ia} + \tau_i^{off} \tag{2}$$

$$\theta_i = \theta_i^{gain}\theta_{ia} + \theta_i^{off} \tag{3}$$

where τ_i^{gain}, τ_i^{off}, θ_i^{gain} and θ_i^{off} are the gains and offsets of the joint i torque and position sensors. τ_{ia} and θ_{ia} are the actual torque and position sensor reading. The true values are τ_i and θ_i.

2.1 Calibration of torque sensor bias and position sensor gain

First we move all joints except i to their mechanical stops. When joint i rotates, the center of gravity (COG) of all distal links and loads is defined as $\mathbf{r}_{i-1}$ when the joint i is at its initial position, say $\theta_i = 0$:

$$\mathbf{r}_{i-1} = \begin{bmatrix} r_{i-1}s\eta_{i-1}c\xi_{i-1} \\ r_{i-1}s\eta_{i-1}s\xi_{i-1} \\ r_{i-1}c\eta_{i-1} \end{bmatrix} \tag{4}$$

where r_{i-1} is the vector length and angles η_{i-1} and ξ_{i-1} are defined in Figure 1.

When the joint i rotates to position θ_i, the torque exerted on the joint to compensate for gravity is:

$$\tau_i = m\mathbf{z}_{i-1} \cdot (^{i-1}\mathbf{g} \times (Rot_z(\theta_i)\mathbf{r}_{i-1})) \tag{5}$$

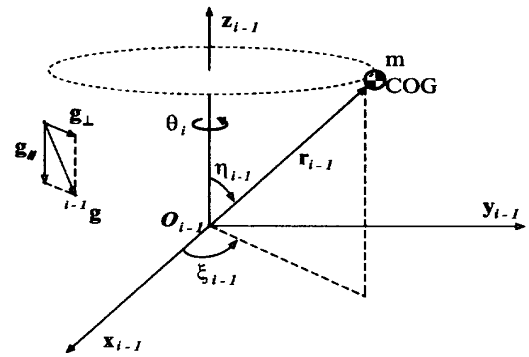

Figure 1: Rotating one joint in the gravity field.

where $Rot_z(\theta_i)$ is the rotation matrix about the $\mathbf{z}_{i-1}$ axis and $Rot_z(\theta_i)\mathbf{r}_{i-1}$ defines the COG when the rotation angle is θ_i. All vectors are expressed in the $i-1$ coordinates. Substituting for $Rot_z(\theta_i)$ and $^{i-1}\mathbf{g} = [^{i-1}g_x \ ^{i-1}g_y \ ^{i-1}g_z]^T$, (5) is expanded as:

$$\begin{aligned} \tau_i &= mr_{i-1}\sqrt{^{i-1}g_x^2 + {}^{i-1}g_y^2}sin(\eta_{i-1}) \\ &\quad sin(\theta_{i-1} + \xi_{i-1} - \gamma_{i-1}) \end{aligned} \tag{6}$$

where $tan\gamma_{i-1} = (^{i-1}g_y/^{i-1}g_x)$.

As shown in Figure 1, $^{i-1}\mathbf{g}$ can be decomposed into one component $\mathbf{g}_\parallel$ along the $\mathbf{z}_{i-1}$ axis and another $\mathbf{g}_\perp$ perpendicular to it. As the joint torque sensor only measures the torque about the joint rotation axis, only $\mathbf{g}_\perp$ contributes to τ_i. This is true if we note that $g_\perp = \sqrt{^{i-1}g_x^2 + {}^{i-1}g_y^2}$, so (6) can be simplified as:

$$\tau_i = A_i sin(\theta_i + \Phi_i) \tag{7}$$

where $A_i = mr_{i-1}g_\perp s\eta_{i-1}$ and $\Phi_i = \xi_{i-1} - \gamma_{i-1}$.

The sinusoidal relation between τ_i and θ_i is demonstrated in (7). Unfortunately, since both $^{i-1}\mathbf{g}$ and $\mathbf{r}_{i-1}$ are not known, the constants A_i and Φ_i are unknown and thus it is impossible to find the torque sensor gain from this equation. However, $^{i-1}\mathbf{g}$ may be solved for later.

Equation (7) is the basis to determine the joint torque sensor offsets and position sensor gains. Followed by (2) and (7), τ_i is given by:

$$\tau_i = \tau_i^{gain}A_i sin(\theta_i^{gain}\theta_{ia} + \theta_i^{off} + \Phi_i) + \tau_i^{off} \tag{8}$$

Since A_i and Φ_i are not known here, we can only solve for θ_i^{gain} and τ_i^{off} by means of sinusoidal curve fitting from actual sensor readings τ_{ia} and θ_{ia}. θ_i^{gain} expands or shrinks the curve along the θ direction, while τ_i^{off} is just the offset of the sinusoidal curve.

The calibration of torque sensor gains and joint angle offsets requires knowledge of the gravity vector. Next we will demonstrate how to solve for $^0\mathbf{g}$ and then proceed to find the torque sensor gains and position sensor offsets. Since we have found θ_i^{gain} and τ_i^{off}, we now assume that both torque sensor bias and rotation angle distortion have been corrected from the sensor readings.

2.2 Solving for the gravity vector in the base coordinates

Let ${}^0\mathbf{g} = [{}^0g_x \; {}^0g_y \; {}^0g_z]^T$ be the gravity vector expressed in the base coordinates. The three components of ${}^0\mathbf{g}$ are constrained by:

$$ {}^0g_x^2 + {}^0g_y^2 + {}^0g_z^2 = 9.8^2 \tag{9} $$

To find ${}^0\mathbf{g}$, we begin by rotating joint 1 to θ_1, then rotating joint 2 in steps for its full range while keeping the first joint stationary. As the gains of the joint position sensors have been found in the previous section, the rotation angle of joint 1 is known exactly following the base coordinates definition. The torque sensor reading from joint 2 is derived from (6):

$$ \tau_2 = C\sqrt{({}^1g_x)^2 + ({}^1g_y)^2}\,sin(\theta_2 + \xi_1 - \gamma_1) \tag{10} $$

where C and ξ_1 are unknown constants related to link mass and COG, torque sensor gain and joint angle offset. ${}^1\mathbf{g} = [{}^1g_x \; {}^1g_y \; {}^1g_z]^T$ is related to ${}^0\mathbf{g}$ by ${}^1\mathbf{g} = {}^1R_0 \; {}^0\mathbf{g}$, which is:

$$ {}^1\mathbf{g} = \begin{bmatrix} {}^0g_x c\theta_1 + {}^0g_y s\theta_1 \\ {}^0g_z \\ {}^0g_x s\theta_1 - {}^0g_y c\theta_1 \end{bmatrix} \tag{11} $$

Substitute (11) into (10) and write the equation in the form of (7) with:

$$ A = C\sqrt{({}^0g_x c\theta_1 + {}^0g_y s\theta 1)^2 + ({}^0g_z)^2} \tag{12} $$

$$ \Phi = \xi_1 - tan^{-1}\left(\frac{{}^0g_z}{{}^0g_x c\theta_1 + {}^0g_y s\theta_1}\right) \tag{13} $$

To solve for ${}^0\mathbf{g}$, we need to set joint 1 at two different positions, θ_1^1 and θ_1^2, and record joint 2 sensor readings when it rotates. For θ_1^j, we may find A^j and Φ^j, where $j = 1, 2$. Thus we have two equations:

$$ \frac{A^1}{A^2} = \frac{\sqrt{({}^0g_x c\theta_1^1 + {}^0g_y s\theta_1^1)^2 + ({}^0g_z)^2}}{\sqrt{({}^0g_x c\theta_1^2 + {}^0g_y s\theta_1^2)^2 + ({}^0g_z)^2}} \tag{14} $$

$$ \begin{aligned} \Phi^1 - \Phi^2 &= -tan^{-1}\left(\frac{{}^0g_z}{{}^0g_x c\theta_1^1 + {}^0g_y s\theta_1^1}\right) \\ &\quad + tan^{-1}\left(\frac{{}^0g_z}{{}^0g_x c\theta_1^2 + {}^0g_y s\theta_1^2}\right) \end{aligned} \tag{15} $$

From (9), (14) and (15) three components of ${}^0\mathbf{g}$ can be solved. In practice, instead of finding the analytical solution, we use least-squares optimization with the objective function:

$$ \min_{{}^0\mathbf{g}, C, \xi_1} \sum_{m=1}^{p} (\tau_{2a} - \tau_{2c})^2 \tag{16} $$

where there are p measurement points. τ_{2c} is computed from (10) and (11), and τ_{2a} is the measured torque.

When both amplitude (14) and phase (15) information is employed, only two different positions of joint 1 are required to solve for ${}^0\mathbf{g}$. This makes the procedure effective.

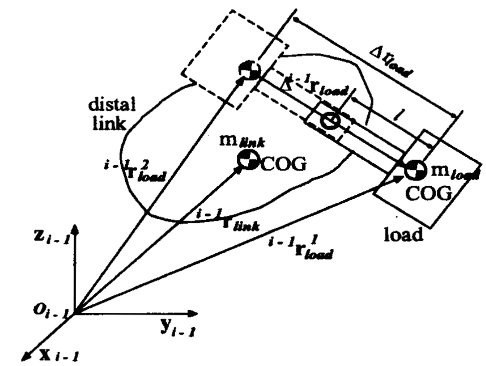

Figure 2: Eliminating the torque due to the link inertia with a known load.

2.3 Torque sensor gain and position sensor offset calibration

When the robot picks up a load, the joint torque exerted to support the robot under gravity consists of two parts: one comes from the link itself and the other comes from the load. Usually link inertial parameter identification requires joint torque information [1]. When calibrating joint torque sensors, we should assume no exact knowledge of link inertial parameters. In fact, these parameters can only be found with calibrated torque and position sensors.

To eliminate the unknown torque due to links, we attach a load whose mass and COG are known. The difference in joint torque when the load is at a different attachment position is only related to the load itself. This makes it possible to calibrate torque sensor gain statically.

In Figure 2, a load with mass m_{load} is attached to one link distal to joint i. The load is preferably attached to the last link so that the torque sensors of all joints except the last one can be calibrated.

In the joint i coordinates, the load COG changes from ${}^{i-1}\mathbf{r}_{load}^1$ to ${}^{i-1}\mathbf{r}_{load}^2$ while ${}^{i-1}\mathbf{r}_{link}$ is unchanged. The torque on joint i is:

$$ \begin{aligned} \tau_i^j &= m_{link}\mathbf{z}\cdot({}^{i-1}\mathbf{g} \times {}^{i-1}\mathbf{r}_{link}) \\ &\quad + m_{load}\mathbf{z}\cdot({}^{i-1}\mathbf{g} \times {}^{i-1}\mathbf{r}_{load}^j) \end{aligned} \tag{17} $$

where $j = 1, 2$ for two load positions and $\mathbf{z} = [0\ 0\ 1]^T$. Subtracting τ_i^1 from τ_i^2, we find the joint torque only due to load position changes.

$$\Delta\tau_i = m_{load}\mathbf{z}\cdot({}^{i-1}\mathbf{g}\times\Delta^{i-1}\mathbf{r}_{load}) \qquad (18)$$

Note in (18) that the vector $\Delta^{i-1}\mathbf{r}_{load}$ is unknown, but its length Δr_{load} is known from the way we change the load position. For example, as we did in our experiment, we bolted the load with m_{load} and l known to the distal link, and changed the load position from ${}^{i-1}\mathbf{r}_{load}^1$ to ${}^{i-1}\mathbf{r}_{load}^2$ (Figure 2). The Δr_{load} in this case is easily found to be $2l$, where l is the distance from the load COG to the bolt center. l is derived from the load model developed with AutoCAD^{TM}.

To calibrate joint i, the procedure is similar to that of finding ${}^0\mathbf{g}$. During the calibration, all other joints except i and $i+1$ are pushed against their mechanical stops with a bias torque. Move joint i to two different positions. For each joint i position, rotate joint $i+1$ in steps for its full range. This time we will observe the torque on joint i instead of joint $i+1$.

$$\Delta\tau_i = m\mathbf{z}\cdot({}^{i-1}\mathbf{g}\times({}^{i-1}R_i(\theta_i)Rot_z(\theta_{i+1}))\Delta\mathbf{r}_{i-1})) \qquad (19)$$

where ${}^{i-1}R_i$ and $\mathbf{r}_{i-1}$ are defined in (1) and (4), and m is the load mass. The expansion of (19) yields:

$$\Delta\tau_i = a_1 sin(\theta_{i+1}+\xi_{i-1})+a_2 cos(\theta_{i+1}+\xi_{i-1})-a_3 \qquad (20)$$

with

$$\begin{aligned} a_1 &= m\Delta r_{i-1}s\eta_{i-1}c\alpha_i({}^{i-1}g_x c\theta_i + {}^{i-1}g_y s\theta_i) \qquad (21)\\ a_2 &= m\Delta r_{i-1}s\eta_{i-1}({}^{i-1}g_x s\theta_i - {}^{i-1}g_y c\theta_i)\\ a_3 &= m\Delta r_{i-1}c\eta_{i-1}s\alpha_i({}^{i-1}g_x c\theta_i + {}^{i-1}g_y s\theta_i) \end{aligned}$$

(20) shows that $\Delta\tau_i$ is a sinusoidal function of θ_{i+1} with $\sqrt{a_1^2+a_2^2}$ as amplitude and a_3 as the offset. Because of this offset, the torque sensor gain can be calibrated.

We proceed from the first joint to the last one. For joint 1, it is simpler as no offset exists for this joint; i.e., θ_1 is known exactly. Thus only one position of joint 1 is required as ${}^0\mathbf{g}$ has also been found. Here $a_1 = 0$ as $\alpha_1 = \pi/2$. a_2 and a_3 become:

$$\begin{aligned} a_2 &= m\Delta r_0 s\eta_0({}^0g_x s\theta_1 - {}^0g_y c\theta_1) \qquad (22)\\ a_3 &= m\Delta r_0 c\eta_0({}^0g_x c\theta_1 + {}^0g_y s\theta_1) \end{aligned}$$

Actually, a_2 and a_3 are scaled by τ_1^{gain} and we will get a_2' and a_3', but the ratio of a_2' and a_3' is the same as that of a_2 and a_3. From the ratio we can find η_0; thus τ_1^{gain} is calculated as:

$$\tau_1^{gain} = \frac{a_3'}{a_3} \qquad (23)$$

Figure 3: A load attached to the Sarcos Dextrous Arm.

For joint 2, θ_2^{off} may also be calibrated along with τ_2^{gain}. For each of the two positions of joint 2, we may have one equation about the ratio of a_2' and a_3', which is a function of η_1 and θ_2^{off}. Then η_1 and θ_2^{off} may be solved from two equations by means of numerical optimization method similar to (16). The same procedure may be applied to other joints distal to joint 2.

3 Experiment results

3.1 Sarcos Dextrous Arm

The Sarcos Dextrous Arm is a ten degree-of-freedom (DOF) hydraulically powered anthropomorphic arm which includes a three DOF multipurpose end effector [9]. The arm DOFs are configured with a roll-pitch-roll spherical shoulder joint, a rotary elbow joint and a roll-pitch-yaw spherical wrist. All DOFs are instrumented with joint torque and rotation position sensors. Joint torque is sensed by a metal foil strain gage load cell; full bridge configurations are used to minimize temperature sensitivity and improve noise rejection. The rotation of the arm joints is sensed by Rotary Variable Differential Transducers (RVDTs) and optionally sensed by very high resolution (400,000 counts/rev) optical encoders. The ranges of rotation are 180 degrees for all arm joints except the wrist abduction/adduction DOF.

We begin each experiment after about 15 minutes warmup. For each rotation step, data from the encoder, RVDT and load cell are averaged 200 times and recorded. We have observed the sensor noise for both RVDTs and load cells to be less than 0.1% full scale. The data from the encoder are used to solve for ${}^0\mathbf{g}$. The gains and the offsets of RVDTs and load cells for the first two joints are calibrated.

3.2 Calibration procedure

We followed the procedures outlined in section 2 to calibrate the sensors of the first two joints of Sarcos

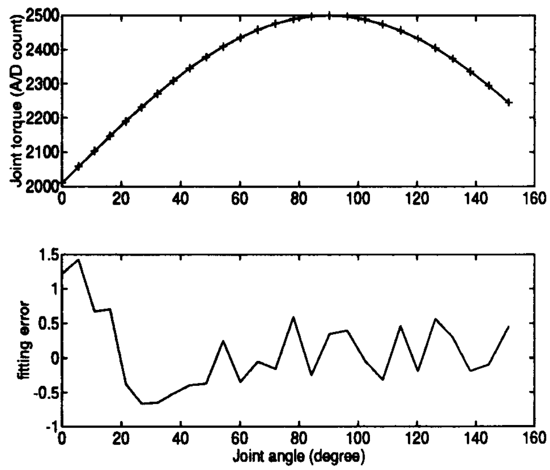

Figure 4: Sinusoidal fitting of experiment data: + for experimental data, solid line for fitted curve.

m_{load}(kg)	l(m)
1.724	0.201

Table 2: Load parameters.

${}^0g_x$	${}^0g_y$	${}^0g_z$
-3.43	-5.94	-7.00

Table 3: Calibrated ${}^0\mathbf{g}$ (m/s^2).

j	τ_j^{gain} (count/(N·m))	τ_j^{off} (count)	θ_j^{gain} (deg/deg)	θ_j^{off} (deg)
1	7.12	2075	0.988	0*
2	5.97	2008	0.995	134.2

Table 4: Calibration results for the first two joints of Sarcos Dextrous Arm: * by definition.

Dextrous Arm. The calibration procedures are summarized here:

Step 1: Calibrate torque sensor offsets and position sensor gains by rotating only one joint at one time while keeping other joints stationary. Record the torque sensor reading and the joint angle, and do sinusoidal curve fitting to find the parameters of this joint.

Step 2: Solve for ${}^0\mathbf{g}$ with the first two joints.

Step 3: Calibrate torque sensor gains and joint angle offsets for joints 1 and joint 2. As shown in Figure 2, the load is bolted to the distal link of the arm in two positions. To calibrate joint i ($i = 1, 2$), torque readings for joint i and position data for both joint i and $i+1$ are recorded when joint $i+1$ rotates statically from one stop to another. This process is done for each load attachment position. Sinusoidal function fitting is made prior to subtracting the torque due to link inertia using equation (17) and (18).

The function fitting in the third step is necessary because the torque due to the link can only be eliminated if the torque sensor of joint i is sampled at the same θ_{i+1} for each of the two load positions when joint $i+1$ rotates, which is not practical for experimental conditions. Subtraction between two fitted sinusoidal functions solves this problem.

3.3 Results

Table 2 shows the parameters of the load we used in the experiment. They are defined in Figure 2. Sinusoidal curve fitting of experiment data is shown in Figure 4. The maximum error between the measured data and fitted data is about 2 counts. Table 3 shows the calibrated ${}^0\mathbf{g}$. The calibration results of the joint torque and position sensors for the first two joints are given in Table 4.

When we installed the Sarcos Dextrous Arm in our laboratory, we found both the gains and the offsets of the RVDTs have shifted from the calibrated values given in the manual by about 5% . The RVDT had been recalibrated using the manual procedure described in [11] before our calibration experiment.

For the Sarcos Dextrous Arm, the +/− 10 V torque sensor analog output is converted with a 12-bit A/D to give 0 to 4096 counts, where 2048 counts correspond to 0 V sensor output. The torque sensor gains of the first two joints were rated as 6.69 (count/(N·m)) by the manufacturer. Our calibration results show a difference of about 10% from the rated gains. We are going to implement other calibration methods and the results here may be verified later.

4 Discussions

This paper has proposed a gravity based autonomous procedure to calibrate the joint torque sensors for robot manipulators. As a by product, the gravity vector is determined and the joint angle gains and offsets can also be determined. The basic idea behind these procedures is the sinusoidal relationship between joint torque and joint position. We found the torque sensor bias and position sensor gain from a biased and horizontally distorted sinusoidal curve. Gravity in the base coordinates is solved from the amplitude and the phase information of two fitted sinusoidal functions. Again, in the calibration of torque sensor gain and position sensor offset, we showed how they are related to the amplitude and the offset of the sinusoidal functions. The sinusoidal function fitting is the basic tool through this paper.

For the position sensor calibration, as the Sarcos Dextrous Arm has intrinsic high precision encoders in addition to RVDTs for the upper five DOFs, one may find the RVDT position sensor gains can be calibrated from the encoder readings. However, for other joints and for other manipulators without high precision encoders, the procedure proposed in this paper will be found useful as a routine procedure.

In the calibration of torque sensor bias and position sensor gain, which is a regular routine for manipulator maintenance, we found the procedure effective in the sense that only one joint was rotating at one time while other joints are kept stationary by applying a biased torque to push them against their stops. This ensures that the torque reading of the rotating joint only comes from gravity and the sinusoidal curve may be obtained in this way (Figure 4).

Movement of two joints is required when calibrating the gravity vector and the torque sensor gains. For the robot without joint brakes (like the Sarcos Dextrous Arm), it is difficult to keep one joint stationary while the other one is rotating. Instead of solving the equations analytically, we used the numerical optimization method to solve for the parameters. In this way, the deflection of the stationary joint is incorporated into the objective function and the results are guaranteed.

As for the drawbacks, this method can not determine the torque sensor gain and position sensor offset of the last joint. A load with known mass and COG must be attached to the manipulator when calibrating the torque sensor gain, which makes the method less autonomous. We are investigating alternative calibration methods; then the calibration results from this procedure may be verified with other procedures.

Acknowledgements

Support for this research was provided by Office of Naval Research Grant N00014-90-J-1849, and by the Natural Sciences and Engineering Research Council (NSERC) Network Centers of Excellence Institute for Robotics and Intelligent Systems (IRIS). Personal support for JMH was provided by the NSERC/Canadian Institute for Advanced Research (CIAR) Industrial Chair in Robotics.

References

[1] An, C.H., Atkeson, C.G., and Hollerbach, J.M., *Model-Based Control of a Robot Manipulator.* Cambridge, MA: MIT Press, 1988.

[2] Canepa, G., Hollerbach, J.M., and Boelen, A.J.M., "Kinematic calibration by means of a triaxial accelerometer," in *Proc. IEEE Intl. Conf. Robotics and Automation*, San Diego, May 8-13, 1994.

[3] Denavit, J., and Hartenberg, R.S., "A kinematic notation for lower pair mechanisms based on matrices," *J. Applied Mechanics*, vol. 22, pp. 215-221, 1955.

[4] Giugovaz, L., and Hollerbach, J.M., "Closed-loop kinematic calibration of the Sarcos Dextrous Arm," in *Proc. IEEE/RSJ Intl. Conf. on Intelligent Robots and Systems*, Munich, submitted, Sept. 12-16, 1994.

[5] Hirose, S., and Yoneda, K., "Development of optical 6-axial force sensor and its signal calibration considering non-linear interference," in *Proc. IEEE Intl. Conf. Robotics & Automation*, Cincinnati, pp. 46-53, May 13-18, 1990.

[6] Hollerbach, J.M., Giugovaz, L., Buehler, M., and Xu, Y., "Screw axis measurement for kinematic calibration of the Sarcos Dextrous Arm," in *Proc. IEEE/RSJ Intl. Conf. on Intelligent Robots and Systems*, Yokohama, pp. 1617-1621, July 26-30, 1993.

[7] Hollerbach, J.M., Hunter, I.W., and Ballantyne, J., "A comparative analysis of actuator technologies for robotics," *The Robotics Review 2*, edited by O. Khatib, J.J. Craig, and T. Lozano-Perez. Cambridge, MA: MIT Press, pp. 299-342, 1992.

[8] Jacobsen, S.C., Smith, F.M., Backman, D.K., and Iversen, E.K., "High performance, high dexterity, force reflective teleoperator II," in *ANS Topical Meeting on Robotics and Remote Systems*, Albuquerque, NM, Feb.24-27, 1991.

[9] Mooring, B.W., Roth, Z.S., and Driels, M.R., *Fundamentals of Manipulator Calibration.* NY: Wiley Interscience, 1991.

[10] Sarcos Reseaech Corporation, *Dextrous Teleoperation System Manual.* Salt Lake City, Utah: Sarcos Research Corporation, 1993.